CFD ANALYSIS OF LOW SPEED TURBULENT FLOW PAST A DELTA WING

Abhishek Patil [1], Piloo Raghu Kumar[1], Aditya Kodkani[1] and Sekhar Majumdar[2]
[1]Undergraduate Student, [2]Professor
Department of Mechanical Engineering
Nitte Meenakshi Institute of Technology, Karnataka, INDIA

Abstract

Delta wing has been a subject of intense research since decades due to decades due to inherent characteristics of generating increased nonlinear lift due to vortex dominated flows. Lot of work has been carried out in order to understand the vortex dominated flows on the delta wing. The delta wing is a wing platform in the form of a triangle. Aerodynamics of wings with moderate sweep angle is recognized by the aerospace community as a challenging problem. In spite of its potential application in military aircraft, the understanding of the aerodynamics of such wings is far from complete. In order to address this situation, the present work is initiated to compute the 3D turbulent flow field over sharp edged finite wings with a diamond shaped planforms and moderate sweep angle. The detailed flow pattern and surface pressure distribution may further indicate the appropriate kind of flow control during flight operation of such wings. The flow field is computed using an in-house developed CFD code RANS3D.

Keywords: Delta Wing, RANS solver, Turbulent Flow

1. Introduction

Computational Fluid Dynamics (CFD) has evolved today as a potential engineering design tool for both internal and external flow in complex arbitrary shaped configuration. A well-validated CFD code can save a lot of design cycle time, cutting down number of tests on similar geometry or under similar flow conditions. The CFD code RANS3D, solving the Reynolds Averaged Navier Stokes (RANS) equations in curvilinear boundary-fitted coordinates for conservation of mass, moment and other scalars in three dimensional turbulent incompressible flows, has already been developed and extensively validated by the present project supervisor and his research group at the CTFD Division, NAL Bangalore during the last two decades.

The Delta Wing shape has the advantage that the leading edge remains behind the shock wave generated by the nose of the aircraft when flying at supersonic speed. A second advantage is that, as the angle of attack is increased, the leading edge vortices are formed and enhance the lift coefficient of the aircraft. The delta wings therefore stall only at a very high angle of attack. . The major focus of the present work is on numerical simulation of 3D turbulent incompressible flow past an isolated backward swept (Sweep Angle = 620) Delta Wing made of a Biconvex Aerofoil section. The computation uses the pressure based finite volume RANS code RANS3D coupled to eddy viscosity based turbulence model and a multiblock structured boundary orthogonal curvilinear grid. Both the grid generation code MESHGEN and the flow solution code RANS3D have been developed recently at NAL Bangalore by the present supervisor and his research group at NAL. The aerodynamic performance of Biconvex Aerofoil section at Re = 0.36×10^6 is estimated from the predicted distribution of the surface pressure and the wall shear stress, derived from CFD analysis for both 2D and 3D configuration.
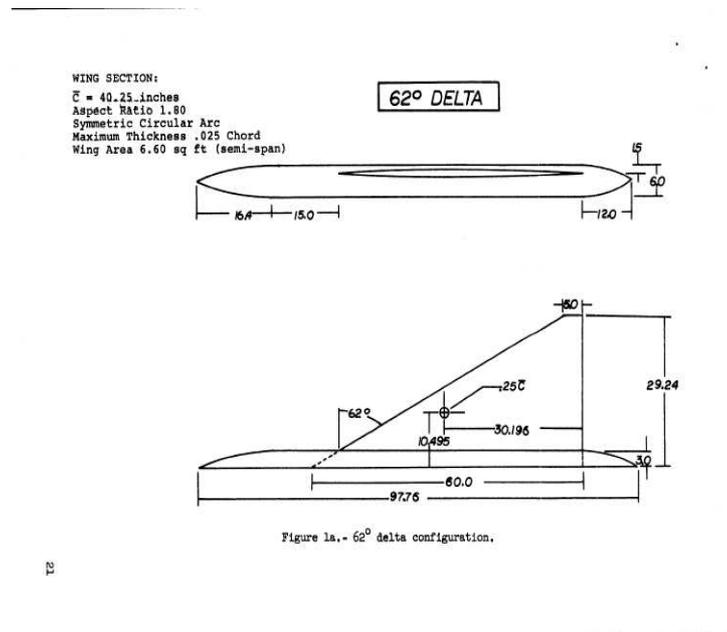
Fig. 1.Configuration for the Delta Wing with a Sweep Angle = 62^0

2. Finite Volume Method

2.1 *Governing Equations of Fluid Motion*

The conservation of mass and momentum equations for turbulent incompressible flow in an inertial frame of reference are expressed by the continuity equation and the Reynolds Averaged Navier Stokes equations respectively. These equations may be written in the following tensor form using general non-orthogonal curvilinear coordinates where j, k and m are the summing indices; μ and ρ are the fluid viscosity and density respectively; and are the time-averaged pressure and cartesian velocity component respectively; ui is the corresponding fluctuating velocity component due to turbulence. J is the transformation Jacobian between the cartesian and the curvilinear coordinates and and are the relevant geometric coefficients related to the transformation

Momentum Conservation :

$$\frac{\partial \overline{U}_i}{\partial t} + \frac{1}{J}\frac{\partial}{\partial x_j}\left[\left(\overline{U}_i\overline{U}_k\beta_k^j\right) - \frac{\nu}{J}\left(\frac{\partial \overline{U}_i}{\partial x_m}B_m^j + \frac{\partial \overline{U}_k}{\partial x_m}\beta_i^m\beta_j^k\right) + \frac{p}{\rho}\beta_i^j + \overline{u_iu_k}\beta_k^j\right] = 0 \quad (1)$$

Mass Conservation : $\quad \frac{\partial}{\partial x_j}\left((\overline{U}_k\beta_k^j) = 0\right. \quad (2)$

2.2 Turbulence Models

The Reynolds Stress tensor is evaluated through appropriate turbulence models. The Linear Eddy Viscosity (LEV) based models, most widely used in RANS computation of complex flows, assume the Reynolds stress tensor components to be directly proportional to the mean strain rates as follows:

$$-\overline{u_iu_k} = \frac{\nu_t}{J}\left(\frac{\partial \overline{U}_i}{\partial x_n}\beta_k^n + \frac{\partial \overline{U}_k}{\partial x_m}\beta_i^m\right) - \frac{1}{3}\delta_{ik}\overline{u_mu_m} \quad (3)$$

where, δ_{ij} is the Kronecker Delta and the subscript m is a summation index. The eddy viscosity ν_t is evaluated

Abhishek Patil ,Piloo Raghu Kumar, Aditya Kodkani , Sekhar Majumdar IJRAME

from the relationship with the local turbulence scalars as following:

$$v_t = C_\mu E_s T_s \qquad (4)$$

where Es and Ts are appropriate energy scale and time scale respectively defining the local turbulence level, and C_μ is a model constant.

In standard k-ε model, used for high Reynolds number flows, proposed originally by Launder & Spalding [6], the eddy viscosity, in Eq. 3 for Reynolds Stress is computed from a turbulence velocity scale and a turbulence length scale which are predicted at each point in the flow via solution of the following transport equations for turbulent kinetic energy and its dissipation rate.

$$D_t k = P_k - \varepsilon + \nabla \cdot \left(\left(v + \frac{v_t}{\sigma_k} \right) \nabla k \right) + D \qquad (5)$$

$$D_t \varepsilon = \frac{C_{\varepsilon 1} P_k - C_{\varepsilon 2} \varepsilon}{T} + \nabla \cdot \left(\left(v + \frac{v_t}{\sigma_\varepsilon} \right) \nabla \varepsilon \right) \qquad (6)$$

Where the eddy viscosity v_t, the turbulent time scale T and the production term P_k are expressed as following in which the S_{ij} denotes the mean strain rate. D_t represents the total derivative of the relevant flow variable with respect to time representing the convective terms

$$v_t = C_\mu k\, T \; ; T = \frac{k}{\varepsilon} \; ; P_k = 2 v_t \left| S_{ij} S_{ij} \right| \; ; S_{ij} = \frac{1}{2} \left(\frac{\partial \overline{U}_i}{\partial x_j} + \frac{\partial \overline{U}_j}{\partial x_i} \right)$$

The model constants are $C_{\varepsilon 1}$ = 1.44, $C_{\varepsilon 2}$ = 1.92, C_μ = 0.09, and the exchange coefficients for the turbulence scalars are

σ_ε = 1.3 and σ_k = 1.0. However these turbulence equations are not strictly valid in the near wall region which needs some special treatment. In the Standard Wall Function method [6], used in the present computation, the first near wall point is assumed to be in the layer where the logarithmic law of wall is used for computation of the mean velocity and the turbulence scalars.

2.3 Numerical Solution of the Finite Volume Equation

Gauss Divergence theorem is used to transform the governing RANS equations (Eq. 1), into the corresponding finite volume analogue in terms of surface flux balance for each control volume. An implicit predictor-corrector method based on a pressure-velocity solution strategy, similar to the SIMPLE Algorithm of Patankar et al [7] is used for numerical solution of the finite volume equation system. Second order accurate Linear Upwind scheme is used for spatial discretisation of the convective fluxes. Using the relevant geometric factors, appropriate discretisation schemes and linearisation of the source terms, the flux balance equations to be solved for momentum and turbulence scalars are expressed in a generalised implicit manner as follows at the predictor step:

$$A_P \phi_P^{n+1} = \left(\sum A_{nb} - SP \right) \phi_P^{n+1} = \sum A_{nb} \phi_{nb}^{n+1} + SU \qquad (7)$$

where, the coefficient A_{nb} represents the combined effect of convection and diffusion at the four faces of a quadrilateral computational cell ; SU and SP are the components of the linearised source term and is the cell volume. In the corrector step, the continuity equation is also transformed to a similar linearised equation for pressure correction in the form of Eq. 7. The corrections for pressure and velocity field obtained are added to the pressure and the momentum-satisfying velocities at the cell centers and cell faces, obtained at the predictor step. The derivation of Eq. 7 and the decoupled iterative procedure to handle the pressure-velocity link are given in details elsewhere [3-5]. The system of linearised equations (Eq. 7) are solved at each outer iteration level using the Strongly Implicit Procedure of Stone [8].

Abhishek Patil ,Piloo Raghu Kumar, Aditya Kodkani , Sekhar Majumdar IJRAME

3. Results and Discussion

The computational and experimental results for turbulent flow around a biconvex delta wing section. Aero foil and also the prediction of three dimensional flow past a finite wing of low aspect ratio of 1.61 with constant biconvex cross section all through the span. The Delta wing of biconvex cross section have been studied mainly for validation of the code "RANS3D" where the present predictions are compared to corresponding measurement data reported in literature [17]. All the computations use the Reynolds Averaged Navier Stokes solver RANS3D for turbulent incompressible flows in complex configuration. The flow solver is provided with six different convective flux discretization schemes and six different turbulence models.

The present 3D computations employ third order accurate quadratic upwind scheme QUICK for discretization of convective flux, coupled to the eddy viscosity based k-ε turbulence model for low Reynolds number flows, proposed by Chien [5]. This turbulence model uses special near-wall exponential damping functions, which allow the eddy viscosity to reduce from its local turbulence-dependent value in the boundary layer to zero on the wall. The objective of these computations is twofold:

(1) To assess the performance and accuracy of the RANS3D code in predicting turbulent incompressible flow past biconvex delta wing sections.

(2) To predict the aerodynamic performance of biconvex delta wing cross section.

The prediction results are compared to available measurement data for the chord wise distribution of surface pressure and also for the variation of aerodynamic coefficients like lift, drag and pitching moment coefficients at different angles of attack. Two dimensional flow patterns around the biconvex delta wing and the corresponding pressure and turbulence energy field for different angle of attacks have also been presented. Flow past a three dimensional wing having biconvex delta wing profile and a rectangular planform with aspect ratio of 1.61 is computed to demonstrate the capability of the 3D flow code The flow results are discussed with adequate physical explanation to justify the prediction results.

The present computation uses H-Grid topology where the wall normal distance of the first near wall grid point is maintained at the order of 1.67x10-5 C for a reasonable resolution of the boundary layers at the operating flow Reynolds number of 0.36 million. The oncoming flow is assumed to be uniform with constant values of the turbulence kinetic energy (k) and its dissipation (ε) decided by the assumption that the turbulence level is 0.1% and the eddy viscosity level is ten times the laminar viscosity of the fluid.
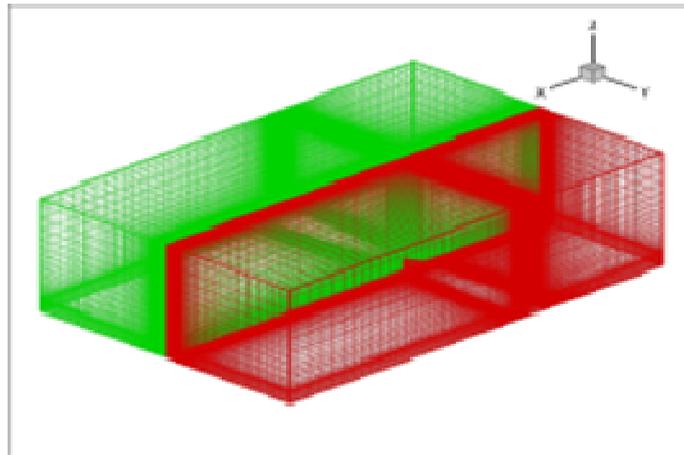

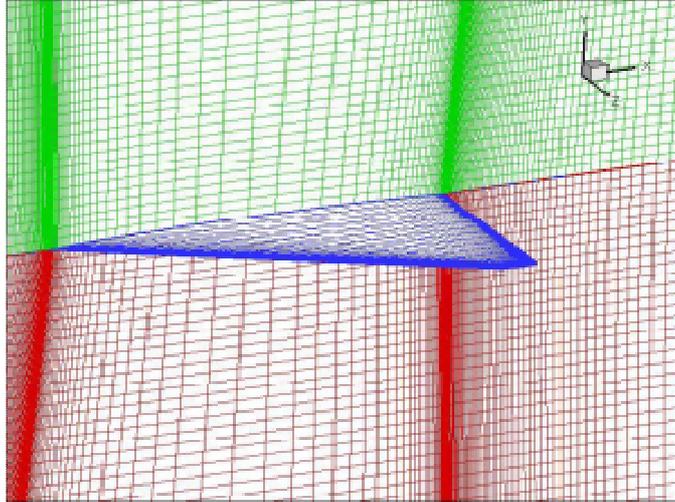*Fig. 2. H grid topology around Aerofoil*

Abhishek Patil ,Piloo Raghu Kumar, Aditya Kodkani , Sekhar Majumdar IJRAME

Fig 3. Zoomed view near the aerofoil

3.1 Numerical Convergence

The transport equations are solved in RANS3D to satisfy the convergence criterion at each time step for the time accurate solution. In case of steady state problems however, one single large time-step is used so that the contribution of the unsteady term is reduced to zero and all the equations are solved iteratively up to the prescribed convergence limit. A convergence criterion of 10^{-5} is used in the present study for the maximum
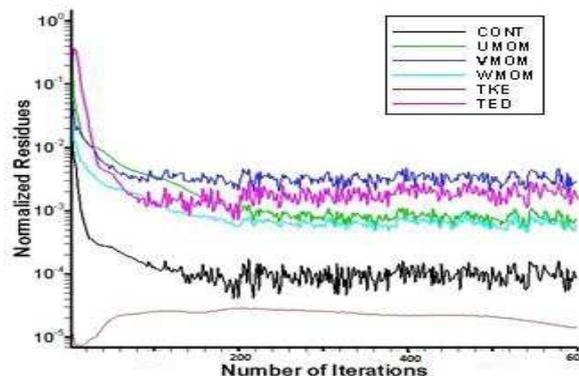

Figure. 4. Numerical convergence history for simulation of flow pas biconvex delta wing

normalized residue of the equations solved and similar behavior of the convergence process has been demonstrated by all the problems studied in the present work. The convergence history is shown in the form of variation of the L2 Norm of the normalized residues (logarithmic scale) of each equation solved, versus the number of iterations for the computation of 3D flow past a Biconvex Delta Wing aero foil. The numerical convergence process for the continuity, for the two relevant momentum equations and for the two transport equations for scalars k and ε are observed to be more or less oscillatory whereas the residues decay by almost four decades in about 532 iterations.

3.2 Flow pattern around the aero foil

Abhishek Patil ,Piloo Raghu Kumar, Aditya Kodkani , Sekhar Majumdar IJRAME

Figs.5 shows the flow pattern around the aero foil section. The pictures show the particle traces or streamlines plotted using the Tecplot360 software, based on the computed velocity vectors for the flow past Biconvex Delta Wing at Four different angles of attack. In each case, the flow is observed to hit the aero foil at the so-called stagnation point near the leading edge and divided into two streams – one along the upper and the other along the lower surface of the aero foil. Further the stagnation point moves upwards or downwards from the leading edge as the angle of attack changes to negative or positive values respectively. The flow is observed to remain attached all over the upper and lower surface of the aero foil for all the four angles of attack before the stalling condition.
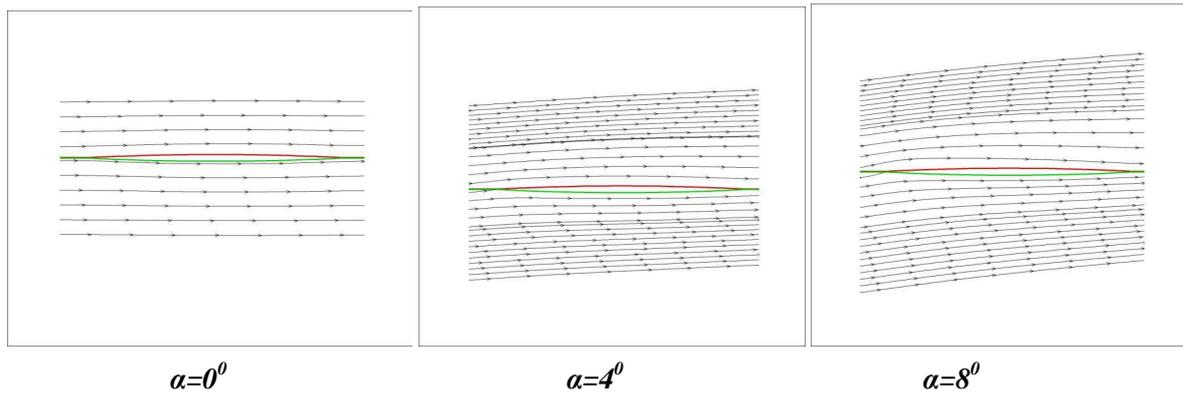

$\alpha=0^0$ $\alpha=4^0$ $\alpha=8^0$

Figure 5(a): Streamline traces with different angles of attack (Re=0.36x10^6)
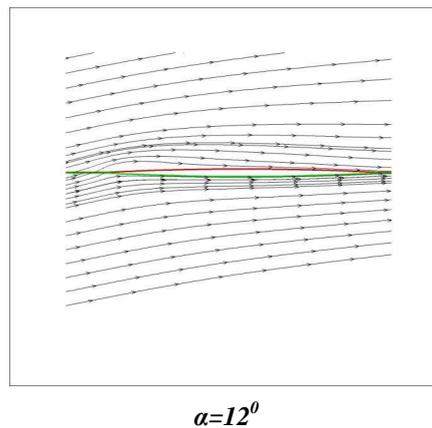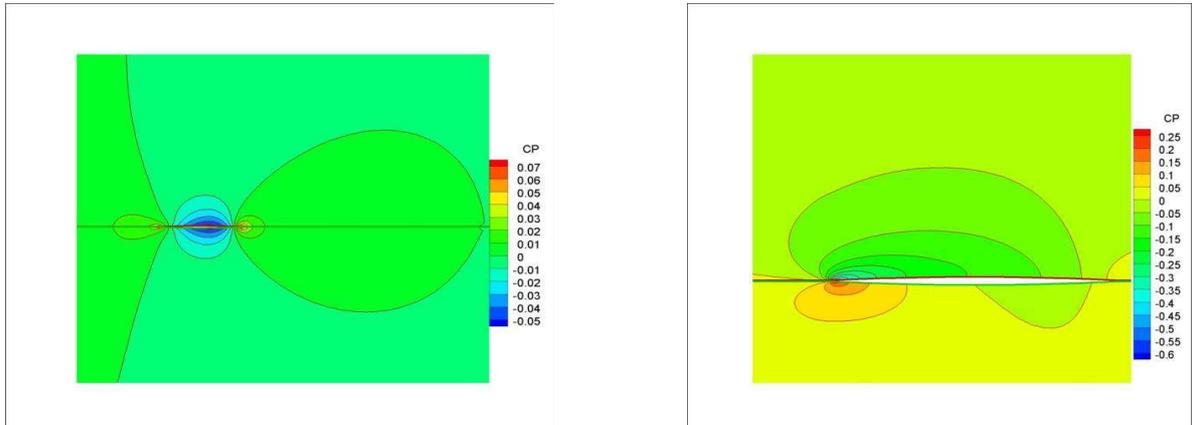

$\alpha=12^0$

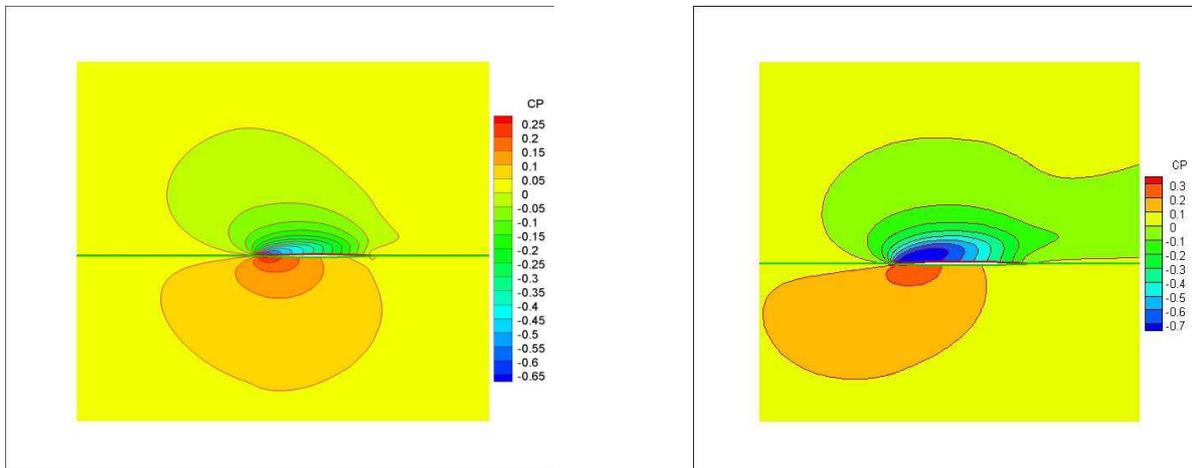**Figure 5(b): Streamline traces (Re=0.36x10^6)**

3.3 Pressure field around the biconvex delta wing

Fig.6 & 7 shows the contours of constant pressure (Cp) around the aero foil for flow at different angles of attack. The pressure contours for zero angle of attack clearly demonstrate the symmetry of the flow for symmetric aero foil. The highest pressure level at the stagnation point near the leading edge is also observed in the pressure contour plots. The contours also deviate from their symmetric pattern when the angle of attack is non-zero. The flooded color contours also demonstrate clearly the negative pressure value bands on the upper surface and positive pressure values on the lower surface of the aero foil.
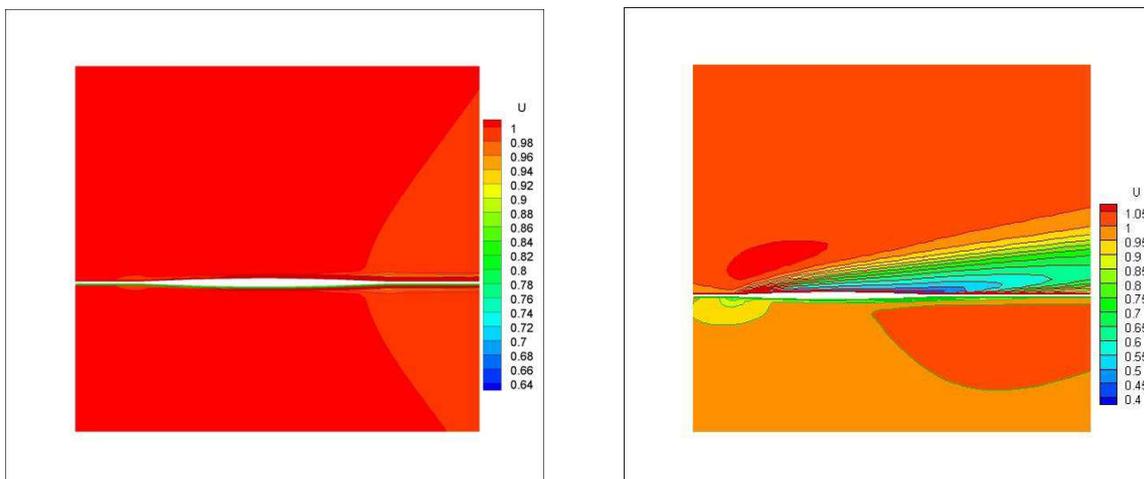
Abhishek Patil ,Piloo Raghu Kumar, Aditya Kodkani , Sekhar Majumdar IJRAME

α=0⁰

α=4⁰

α=8⁰

α=12⁰

Figure 6: Predicted Pressure contours with different angles of attack
(Re=0.36x10⁶,,z/Croot =0.27(mid- section))

α=0⁰

α=4⁰

Abhishek Patil ,Piloo Raghu Kumar, Aditya Kodkani , Sekhar Majumdar

α=8⁰ α=12⁰

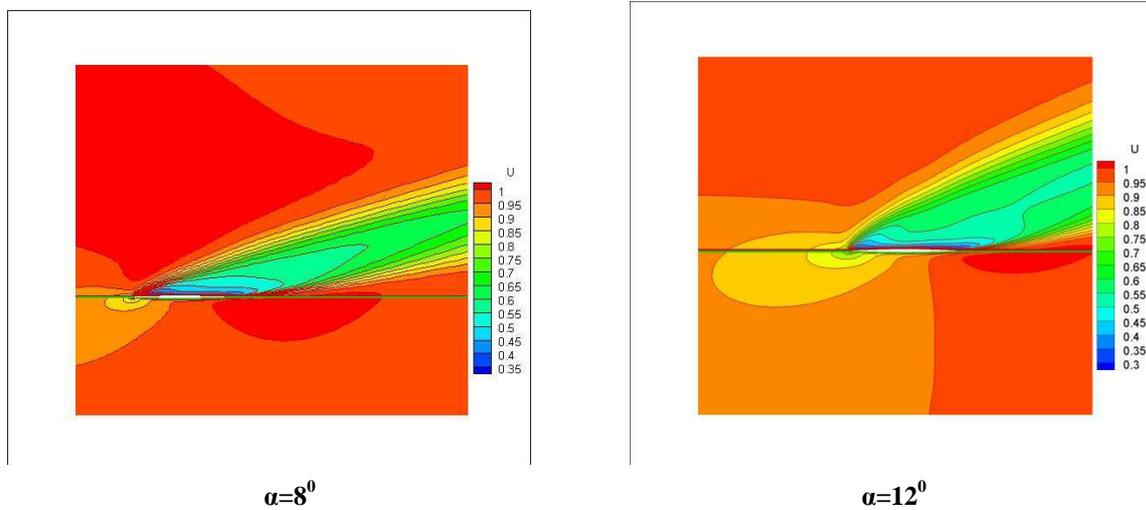*Figure.7. Predicted pressure contours with different angles of attack*
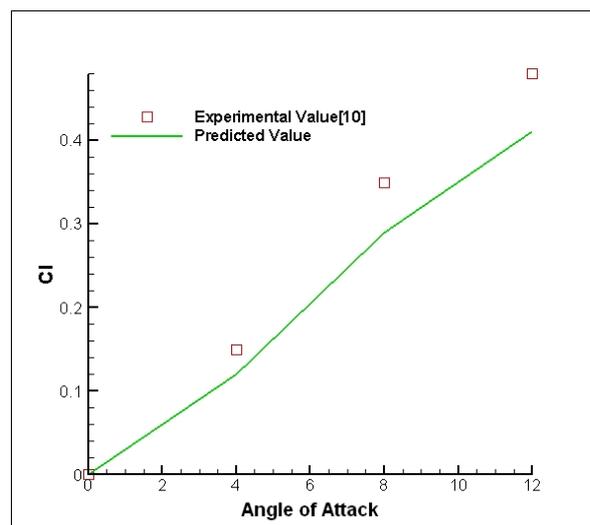*(Re=0.36x10⁶, z/C=0.45(Tip))*

Figure.8. Variation of C_L vs Angle of Attack (α)

4. CONCLUDING REMARKS

1. The computation of flow past a biconvex delta wing cross section with aspect ratio 1.61 shows physically possible flow field, demonstrated by the surface pressure distribution and particle traces on different planes.

2. 3D grid around an isolated backward swept Delta Wing (Sweep Angle = 62⁰) is generated by parallel stacking (along spanwise direction z) of the 2D Grid generated by MESHGEN at the root cross section (Biconvex) plane (x-y) of the wing. Beyond the wing tip, the grid planes along the root chord from the upper and lower blocks of the grid are collapsed on a single plane (y=0).

Abhishek Patil ,Piloo Raghu Kumar, Aditya Kodkani , Sekhar Majumdar IJRAME

3. The mathematical background and coding of the elliptic grid generator MESHGEN used especially for generating curvilinear boundary-fitted grid for the biconvex wing cross section, has been thoroughly understood in details.

4. The relative performances of different sections are assessed by comparing their surface pressure distribution, skin friction distribution, flow pattern and variation of aerodynamic coefficients

5. ACKNOWLEDGMENT

6. REFERENCES

[1] Fathima, A., Baldawa, N.S., Pal, S., Majumdar, S. (1994), Grid generation for arbitrary 2D configurations using a differential algebraic hybrid method, NAL PD CF9416, April 1994

[2] Majumdar Sekhar, Rajani B.N., Kulkarni D.S., Subrahmanya M.B. (2009), CFD simulation of low speed turbulent flow problems using Unsteady RANS and Large Eddy Simulation approach, Journal of Aerospace Sciences and Technologies, Special Issue, February 2009

[3] Majumdar S., Rajani B.N., Kulkarni D., Mohan S., (2003), RANS computation of low speed turbulent flow in complex configuration, Proc. Symposium on State of the Art and Future Trends of CFD at NAL   NAL SP 0301

[4] Majumdar S.,(1998) Pressure based Navier Stokes solver for three-dimensional flow in hydrodynamics and low speed aerodynamics applications, Proc. 3rd Asian CFD Conference, Bangalore, December 7-11, 1998

[5] Majumdar S., Rodi W.,and Zhu J.(1992), Three dimensional finite volume method for incompressible flows with complex boundaries, Journal of Fluids Engineering., ASME, pp. 496-503

[6] Launder B.E., Spalding D.B. (1974), The numerical computation of turbulent flows, Computer Methods and Applied Mechanics and Engineering. vol. 3, p. 269

[7] Patankar S.V. (1980) Numerical Fluid Flow and Heat Transfer, Hemisphere Publishing Corporation, McGraw Hill Book Company

[8] Stone H.L. (1968), Iterative solution of implicit approximations of multidimensional partial differential equations, SIAM Journal of Numerical Analysis, vol. 5, pp. 530-538G.

[9] Chen C. J and Jaw S. Y, (1998), Fundamentals of Turbulence Modeling, Taylor and Francis.

[10] Kulkarni DS, Rajani B N, Majumdar S (2001), Studies on temporal and spatial discretization schemes used in a pressure based RANS algorithm for Incompressible flow, Project Document CF 0108, NAL, Bangalore.

[11] Mansour N. N, Kim J. and Moin P., (1988), "Reynolds-stress and dissipation-rate budgets in a turbulent channel flow", Journal of Fluid Mechanics, vol. 194, pp. 15-44

[12] Patankar S. V (1980), "Numerical Heat transfer and fluid flow", Hemisphere publ. Co

[13] Weber C. and Ducros F., Large Eddy and Reynolds Averaged Navier-Stokes simulations of turbulent flow over an aerofoil. IJCFD,13:327.355,2000

[14] Wilcox, (1993), Turbulence modeling for CFD, DCW Industries Inc., California.

[15] Zhu, J (1990), " A hybrid-differential-algebraic method for three-dimensional grid generation ", International Journal for Numerical Methods in Engineering, vol. 29, pp. 1271-1279,

[16] Majumdar S, (1988), Role of Under-relaxation in momentum interpolation for calculation of flow with non-staggered grids, Numerical Heat Transfer, Vol.13, pp 125-132.

[17] William H. Wentz, Jr. and Michael C. McMahon., " An experimental investigation of the flow fields about Delta and Double-Delta wings at low speeds"

Abhishek Patil ,Piloo Raghu Kumar, Aditya Kodkani , Sekhar Majumdar IJRAME